

Full Length Research Paper

A new anti-lipopolysaccharide factor (EsALF-3) from *Eriocheir sinensis* with antimicrobial activity

Leilei Wang^{1,2}, Ying Zhang^{1,2}, Lingling Wang^{1,*}, Jialong Yang^{1,2}, Zhi Zhou^{1,2}, Yunchao Gai^{1,2}, Limei Qiu¹ and Linsheng Song¹

¹Key Laboratory of Experimental Marine Biology, Institute of Oceanology, Chinese Academy of Sciences, Qingdao 266071, China.

²Graduate school, Chinese Academy of Sciences, Beijing 100049, China.

Accepted 23 September, 2011

The cDNA of a new *Eriocheir sinensis* ALF (designated as EsALF-3) was obtained based on EST analysis. The full-length cDNA was of 956 bp, consisting of an open reading frame (ORF) of 369 bp encoding a polypeptide of 123 amino acids. In the deduced amino acid sequence of EsALF-3, there were two highly conserved cysteine residues to define the LPS binding site, and eight positively charged residues existed between the two cysteine residues. The phylogenetic analysis revealed that EsALF-3 was clustered with the ALFs from some crustaceans, forming a separate sister branch to the group of EsALF-1 and EsALF-2 from *E. sinensis*. The mRNA transcript of EsALF-3 was detected in all the examined tissues of crabs, including haemocytes, hepatopancreas, gill, muscle, heart and gonad. The recombinant protein of EsALF-3 represented antimicrobial activity against *Listonella anguillarum*, *Escherichia coli* and *Bacillus subtilis* with minimal inhibitory concentration (MIC) values of 33.75 µg mL⁻¹, 270 µg mL⁻¹ and 135 µg mL⁻¹, respectively. These results together indicated that there were multiple ALF isoforms coexist in *E. sinensis*, and the diversity of the immune effector molecules in innate immune system, such as ALF, helps Chinese mitten crab to deal with various pathogens in the aquatic environment.

Key words: *Eriocheir sinensis*, anti-lipopolysaccharide factor, *Listonella anguillarum*, *Bacillus subtilis*, antimicrobial activity.

INTRODUCTION

Chinese mitten crab, *Eriocheir sinensis*, is one of the most valuable cultivated crustacean species and important food sources in South-East Asia (Ying et al., 2006). In the past years, with the development of intensive culture, various diseases resulted from the infection of bacteria, viruses or rickettsia-like organisms (Zhang et al., 2002; Wang et al., 2004, Wang and Gu, 2002; Wu and Feng, 2004) caused catastrophic economic losses to the crab aquaculture. Like other invertebrates, Chinese mitten crab lacks an acquired immune system and mainly relies on innate immune system to defense invading pathogen. Innate immune system consists of cellular responses including

phagocytosis as well as encapsulation, and humoral immune responses that employ constitutive and inducible Antimicrobial Peptides (AMPs) to lyse invading microorganisms (Hoffmann et al., 1999; Roch, 1999). Characterization of those AMP immune effectors and understanding the immune defense mechanisms of crustacean species may be contributed to the development of management strategies for disease control in crab aquaculture.

Antimicrobial peptides (AMPs) are a group of effector molecules characterized by their small-size, heat-stability and broad spectrum of antimicrobial activity against bacteria, fungi, as well as viruses and eukaryotic parasites (Boman, 2003). They are important components of the host innate immune response against microbial invasion. These peptides share certain common similarities in structural patterns or motifs, and the most

*Correspondence author. E-mail: wanglingling@ms.qdio.ac.cn.
Tel: 86-532-82898552. Fax: 86-532-82880645.

prominent structures are amphiphilic peptides with two to four β -strands, amphipathic α -helices, loop structures and extended structures (Boman, 1995; Hancock, 1997; Jenssen et al., 2006). A variety of AMPs have been identified and characterized in all living kingdoms, from bacteria to human. According to the structural characteristics, these AMPs can be classified into three major groups such as:

- (i) Peptides with an α -helical conformation (insect cecropins, magainins, etc.).
- (ii) Cyclic and open-ended cyclic peptides with pairs of cysteine residues (defensins, protegrin, etc.)
- (iii) Peptides with an over-representation of some amino acids (proline rich, histidine rich, etc.) (Bachere et al., 2004; Bulet et al., 2004).

Several types of AMPs have been so far found and characterized in crustacean species such as penaeidins, callinectin, carcinin, proline rich peptide and anti-lipopolysaccharide factors (ALFs) (Destoumieux et al., 1997; Khoo et al., 1999; Relf et al., 1999; Schnapp et al., 1996; Tanaka et al., 1982).

As an important member of AMP family, ALF is a small amphipathic protein containing a conserved disulfide loop which can bind and neutralize lipopolysaccharide (LPS), mediating degranulation and activation of an intracellular coagulation cascade (Morita et al., 1985; Warren et al., 1992). The first ALF, named LALF, was identified from the amoebocyte of horseshoe crab *Limulus polyphemus* (Morita et al., 1985; Tanaka et al., 1982). Two highly conserved-cysteine residues had been found in the LPS binding domain of LALF after crystal structure analysis (Hoess et al., 1993; Ried et al., 1996). The region responsible for LPS binding in LALF was characterized by an alternating series of positively charged and hydrophobic residues which formed a positively charged amphipathic loop (Ried et al., 1996). A cyclic peptide derived from this region had been reported having preventive and therapeutical effects in a mouse model with peritoneal fulminating sepsis under the LPS attack (Vallespi et al., 2003, 2000). Thereafter, more ALFs have been identified and characterized from crustacean species, such as *Penaeus monodon* (Somboonwiwat et al., 2005), *Fenneropenaeus chinensis* (Liu et al., 2005), *Scylla paramamosain* (Imjongjirak et al., 2007), *Litopenaeus vannamei* (de la Vega et al., 2008), *Litopenaeus schmitti* (Rosa et al., 2008), *E. Sinensis* (Li et al., 2008; Zhang et al., 2010b), *Scylla serrata* (Yedery and Reddy, 2009), *Portunus trituberculatus* (Yue et al., 2010) and so on.

Though the members of ALFs family are structurally similar, they can display different antibacterial spectrum. For example, LALF only displays antibacterial activity on Gram-negative bacteria (Morita et al., 1985), and ALF from *S. serrata* has antibacterial effect on both Gram-negative and Gram-positive bacteria (Yedery and

Reddy, 2009), while the ALF from *P. monodon* has a broad spectrum of antifungal properties against filamentous fungi and antibacterial activities against both Gram-positive and Gram-negative bacteria (Somboonwiwat et al., 2005). Moreover, more than one ALF isoforms was identified in one organism, and they even displayed different biological activities. For example, two ALF isoforms in *L. Vannamei* (LvALF1 and LvALF2) represented different antimicrobial activities (de la Vega et al., 2008). In our previous study, two ALFs (EsALF-1 and EsALF-2) were identified from *E. sinensis*. EsALF-1 displayed antimicrobial activity against both Gram-positive and Gram-negative bacteria, while EsALF-2 displayed antimicrobial activity against Gram-negative bacteria and fungi (Li et al., 2008; Zhang et al., 2010b). Considering the large number of bacteria in the aquatic environment that are pathogenic for crab, it is likely that there are diverse ALFs involved in crab immunity against various pathogen infections. The main objectives of the present study were (1) to characterize the third isoform of ALF from *E. sinensis* (designated as EsALF-3), (2) to study tissue-specific expression of EsALF-3, and (3) to characterize the antimicrobial activity of recombinant EsALF-3 against various bacteria.

MATERIALS AND METHODS

Crabs and tissue collection

Healthy *E. sinensis*, averaging 30 g in weight, were collected from a farm in Qingdao, China, and maintained in aerated freshwater at $23 \pm 2^\circ\text{C}$ for 1 week before processing. During the experiment, the crabs were fed with commercial feed, and water was totally exchanged daily.

Five tissues, including hepatopancreas, muscle, gonad, gill and heart were collected from six healthy adult crabs. Hemolymph from crabs was also collected from the cheliped using a syringe with an equal volume of anticoagulant (100 mM glucose, 26 mM citric acid, 415 mM NaCl, 30 mM sodium citrate, 30 mM EDTA, pH 4.6) (Zhang et al., 2010b), and immediately centrifuged at 800 g, 4°C for 10 min to harvest the haemocytes. All these tissue samples were stored at -80°C after addition of 1 ml TRIzol reagent (Invitrogen) for subsequent RNA extraction.

RNA isolation and cDNA synthesis

The total RNA was isolated from different tissues of crabs using TRIzol reagent (Invitrogen). Briefly, 0.2 mL of chloroform was added to the previously incubated samples with TRIzol (Invitrogen) for 5 min at room temperature. Then the tube was shaken vigorously by hand for 15 s and incubated for 2 min at room temperature. The tubes were centrifuged at $12,000 \times g$ for 15 min at 4°C ; the aqueous phase of the sample was pipetted to another new tube with 0.5 mL of 100% isopropanol and incubated at room temperature for 10 min.

Then the tubes were centrifuged at $12,000 \times g$ for 10 min at 4°C , and the supernatant was discarded. Later, 1 mL of 75% ethanol was added to wash the pellet, and centrifuged at $7,500 \times g$ for 5 min at 4°C . The RNA pellet was air dried for 5 min, and resuspended in 20 μL RNase-free water for cDNA synthesis.

The first-strand cDNA synthesis was carried out based on Promega M-MLV RT Usage information using the DNase I

(Promega)-treated total RNA as template and oligo (dT)-adaptor as primer (Table 1). The reaction mixtures were incubated at 42°C for 1 h, and then terminated by heating at 95°C for 5 min. The cDNA mix was diluted to 1:100 and stored at -80°C for following process.

Cloning the full-length cDNA of EsALF-3 based on EST

A cDNA library was constructed from the haemocytes of Chinese mitten crab challenged by a mixture of *L. anguillarum* and *Staphylococcus aureus*. Random sequencing of the library yielded 7535 ESTs (Gai et al., 2009). BLAST analysis revealed that one EST of 956 bp was highly similar to previously identified anti-lipopolysaccharide factor from crustaceans and contained full-length cDNA sequence. Two specific primers P1 and P2 (Table 1) were designed based on the EST sequence to check the full-sequence cDNA of EsALF-3. The PCR reactions to amplified 3' and 5' end of EsALF-3 were performed using primers T3 and P1 or P2 and T7 in a 25 µL reaction volume containing 2.5 µL of 10 × PCR buffer, 1.5 µL of MgCl₂ (25 mmol L⁻¹), 2.0 µL of dNTPs (2.5 mmol L⁻¹), 1.0 µL of each primer (10 mmol), 15.8 µL of PCR-grade water, 0.2 µL of Taq polymerase (TaKaRa, 5 U µL⁻¹) and 1 µL of cDNA mix. The PCR temperature profile was 94°C for 5 min, followed by 35 cycles of 94°C for 30 s, 57°C for 30 s, 72°C for 1 min, and the final extension step at 72°C for 10 min. The PCR products were cloned into the pMD18-T simple vector (TaKaRa) and sequenced in both directions with primers M13-47 and RV-M (Table 1). The sequencing results were verified and then subjected to cluster analysis.

Sequence analysis, multiple sequences alignment, tertiary structures prediction and phylogenetic analysis of EsALF-3

The homology searches of nucleotide and protein sequences were conducted with BLAST algorithm at the National Center for Biotechnology Information (<http://www.ncbi.nlm.gov/blast>). The deduced amino acid sequence was analyzed with the Expert Protein Analysis System (<http://www.expasy.org>). SignalP 3.0 program was utilized to predict the presence and location of signal peptide, and the cleavage sites in amino acid sequences (<http://www.cbs.dtu.dk/services/SignalP>).

The ClustalW Multiple Alignment program (<http://www.ebi.ac.uk/clustalw/>) was used to create the multiple sequence alignment. The presumed tertiary structures were established using SWISSMODEL prediction algorithm (<http://swissmodel.expasy.org/>) and displayed by DeepView/Swiss-Pdb Viewer version 4.01. An unrooted phylogenetic tree was constructed based on the amino sequences alignment by the neighbor-joining (NJ) algorithm embedded in Mega 4 program. The reliability of the branching was tested by bootstrap re-sampling (1000 pseudo-replicates).

Quantitative real-time RT-PCR analysis of EsALF-3 mRNA expression in different tissues

EsALF-3 mRNA expression was detected by SYBR Green fluorescent quantitative real-time PCR (RT-PCR) in an ABI PRISM 7300 Sequence Detection System. The amplifications were conducted in triplicates in a total volume of 50 µL. The EsALF-3 specific primers P3 and P4 (Table 1) were used to amplify the corresponding products. The β-actin from *E. sinensis*, amplified with primers P5 and P6 (Table 1), was chosen as reference gene for internal standardization. After the PCR program, data were analyzed with SDS 2.0 software (Applied Biosystems). To maintain consistency, the baseline was set automatically by the software. The comparative average cycle threshold method was used to analyze the mRNA expression level of EsALF-3, and the value stood for an

n-fold difference relative to the calibrator (Zhang et al., 2010a). All data were given in terms of relative mRNA expressed as mean ± S.E. (N = 5). The data were then subjected to one-way analysis of variance (one-way ANOVA) followed by an unpaired, two-tailed t-test. Difference was considered to be significant at P < 0.05.

Recombinant expression of EsALF-3 and protein purification

The cDNA fragment encoding the mature peptide of EsALF-3 was amplified with specific primers P7 and P8 (Table 1) with BamHI and XhoI sites at their 5' end, respectively. The purified PCR products were inserted into pMD18-T simple vector, and digested with the restriction enzymes BamHI and XhoI. Then the fragments were inserted into the BamHI/XhoI sites of vector pET-32a (+) (Novagen) to generate pET-32a-EsALF-3 recombinant which was sequenced by the primers of P7 and P8 to ensure in-frame insertion. The recombinant plasmid was transformed into *E. coli* BL21 (DE3)-pLysS (Novagen). Positive clones were screened by PCR reaction with primers P7 and P8 and confirmed by nucleotide sequencing. The pET-32a vector without insert fragment was selected as a negative control, which could express a thioredoxin (Trx) with 6 × His-tag in the prokaryotic expression system. Positive transformants of rEsALF-3 and negative control were incubated in 100 mL SOB medium containing 50 µg mL⁻¹ ampicillin at 37°C with shaking at 220 rpm until the culture reached O.D. 600 of 0.5 to 0.7. Isopropyl-β-D-thiogalactosidase (IPTG) was then added to the medium at a final concentration of 1 mmol L⁻¹. The recombinant EsALF-3 protein (rEsALF-3) was purified by nickel affinity chromatography MagExtractor His-Tag NPK-700 (Toyobo) as described by the manufacturer. The resultant protein was separated electrophoretically on 15% SDS-polyacrylamide gel (SDS-PAGE) according to the method of Laemmli (Laemmli, 1970) and visualized with Coomassie brilliant blue R250. The purified protein was refolded using a linear 6 to 0 M urea gradient in 50 mmol L⁻¹ Tris-HCl, pH 7.4, 50 mmol L⁻¹ NaCl, 10% glycerol, 1% glycine, 1 mmol L⁻¹ EDTA, 0.2 mmol L⁻¹ oxidized glutathione and 2 mmol L⁻¹ reduced glutathione. The concentrations of rEsALF-3 and rTRX protein were measured by BCA (bicinchoninic acid) Protein Assay Kit.

Antimicrobial activity assay

The antimicrobial activity assay was performed according to the method described by Zhang et al. (2010b). Briefly, the microbial strains used in the assays included Gram-negative bacteria *L. anguillarum* and *E. coli*, Gram-positive bacteria *Micrococcus luteus* and *B. subtilis*, and fungus *Pichia pastoris*, which were grown and assayed in marine broth 2216 E at 28°C, fresh LB medium at 37°C, and fresh YPD medium at 30°C, respectively. *L. anguillarum*, *E. coli*, *M. luteus*, *B. subtilis* and *P. pastoris* were grown to mid-logarithmic phase and diluted with Tris-HCl (50 mmol L⁻¹, pH 8.0) to 10³ colony forming units (CFU) mL⁻¹. In sterile 96-well plates, 50 µL of rEsALF-3 starting at approximate 540 µg mL⁻¹ in 1/2-fold serial dilution with Tris-HCl (50 mmol L⁻¹, pH 8.0) were added into the wells. The wells with 50 µL of Tris-HCl (50 mmol L⁻¹, pH 8.0) were used as blank group and 50 µL of rTRX diluted into Tris-HCl (50 mmol L⁻¹, pH 8.0) were used as negative control. In each well, 50 µL of cell suspension (1 × 10³ cells mL⁻¹) were added and the 96-well plates were incubated at corresponding temperatures for up to 3 h, and then 150 µL of corresponding growth medium were added. After the mixtures were cultured at corresponding temperatures overnight, the absorbance at 600 nm for bacteria or 560 nm for fungus of each well was determined using a precision micro-plate reader. Each experiment was repeated in quadruplicate and all data were subjected to the unpaired two-tailed student's test and one-way analysis of variance (ANOVA). Differences were considered to be statistically significant at a P value of 0.05 or less.

Table 1. Names and sequences of primers used in this study.

Primer name	Sequence
Oligo(dT)-adaptor	5'-GGCCACGCGTCGACTAGTAC(T)17-3'
Clone primers	
T3	5'-AATTAACCCTCACTAAAGGG-3'
T7	5'-GTAATACGACTCACTATAGGGC-3'
P1	5'-TGGCACAACGACACCGTGGACT-3'
P2	5'-CGCCTCGGTGATGAGTCCCTT-3'
RT primers	
P3 (forward)	5'-GACGAGGAAGTAGGCTTAGTGGT-3'
P4 (reverse)	5'-GGGCTGCTGTTCTCTCTGGA-3'
β -Actin primers	
P5 (forward)	5'-GCATCCACGAGACCACTTACA-3'
P6 (reverse)	5'-CTCCTGCTTGCTGATCCACATC-3'
Recombination primers	
P7 (forward)	5'-GGATCCCAGTGGCAAGCCCTGGTGG-3'
P8 (reverse)	5'-CTCGAGTTAGATCTTGAGCCAGAGTTTTGC-3'
Sequencing primer	
M13-47 (forward)	5'-CGCCAGGGTTTTCCAGTCACGAC-3'
RV-M (reverse)	5'-GAGCGGATAACAATTTACACAGG-3'

RESULTS

cDNA cloning and sequence characterization of EsALF-3

A 956 bp nucleotide sequence representing the complete cDNA sequence of EsALF-3 was obtained by random sequencing of the cDNA library using T3 primer (Table 1), which was then confirmed by overlapping the corresponding EST with the fragments amplified with specific primers of P1 and T3, P2 and T7. The sequence was deposited in GenBank under accession number HQ850572. The complete sequence of EsALF-3 cDNA containing a 5' untranslated region (UTR) of 196 bp, a 3' UTR of 388 bp with a poly (A) tail, and an open reading frame (ORF) of 369 bp encoding a polypeptide of 123 amino acids with the predicted theoretical isoelectric point of 9.10. The nucleotide and deduced amino acid sequence of EsALF-3 is shown in Figure 1. The N-terminus of EsALF-3 had the consistent features with a signal peptide as defined by SignalP program, with a putative cleavage site located after position 26 (CEA-QW).

Homologous and phylogenetic analysis of EsALF-3

Sequence similarity between EsALF-3 and other

members of ALF Family was revealed by BLAST analysis. EsALF-3 shared higher similarity with ALFs from *P. trituberculatus* (67%), *S. serrata* (61%), *Pacifastacus leniusculus* (51%), *Marsupenaeus japonicus* (46%) and *P. monodon* (45%). The similarity between EsALF-3 and two ALFs previously identified from *E. sinensis* was relatively lower (40% for EsALF-1 and 41% for EsALF-2). Multiple sequence alignment revealed that two cysteine residues (C⁵⁵ and C⁷⁶) were highly conserved in EsALF-3, and eight positively charged residues (K⁵⁶, R⁵⁸, R⁵⁹, K⁶², K⁶⁴, R⁶⁵, H⁷⁰ and K⁷³) existed between the two conserved cysteine residues in EsALF-3. Moreover, the consensus pattern of W(T)CPG(S)WT(A) was also identified in EsALF-3 (Figure 2).

To evaluate the molecular evolutionary relationships of EsALF-3 against other ALF family members from crustacean animals, a phylogenetic tree was constructed by the neighbor-joining method (Figure 3). There were generally two distinct groups in the phylogenetic tree, and EsALF-3 fall in the first group consisted of ALFs from crabs *P. trituberculatus* and *S. serrata*, and shrimps *P. leniusculus*, *M. japonicus*, *P. monodon*, *Fenneropenaeus indicus*, *Farfantepenaeus paulensis*, *L. vannamei* and *L. schmitti*. The other two ALFs identified from *E. sinensis*, EsALF-1 and EsALF-2, were clustered in the second group including ALFs from *L. stylirostris* and *Scylla paramamosain*.

```

1  attcgaattcgaattcccaggagtggagcctgcggcttaatttgactcaacacgg
61  ggaacctcaccaggcccagacaccggaaggattgacagattgagagctctttctcgattc
121 ggtgggtgatggtggcaaagcaacgaggagcaaggaaagaaagccgttttgtccttcgcg
1            M R G S V L T G L C V A A V V
181 tcgcagectgaggaccATGAGAGGCAGCGTGTGACCGGCCTGTGTGTGGCGGCGGTGGT
16  L C V Y L P Q P C E A Q W Q A L V G P L
241 GCTCTGTGTGTACCTCCCCAGCCGTGTGAGGCCAGTGGCAAGCCCTGGTGGGACCGCT
36  I E K V S G L W H N D T V D F M G R E C
301 CATTGAAAAAGTCTCTGGTCTATGGCACAACGACACCGTGGACTTCATGGGCCGAGAATG
56  K F R R S P K I K R W E L Y H E G K F W
361 CAAATTCCGCAGGAGCCCCAAAATCAAGCGCTGGGAATTGTACCACGAGGGCAAATTTTG
76  C P G W A P F S G N S S K R S R S G S L
421 GTGTCTGGCTGGGCACCCTTCTCCGGCAATTCTAGCAAGAGGAGCAGATCAGGGTCGCT
96  E E A T R D F V R Q A F E K G L I T E A
481 GGAGGAAGCCACTCGGGACTTCGTGCGTCAGGCCTTCGAAAAGGGACTCATCACCGAGGC
116 D A K L W L K I *
541 GGACGCAAAACTCTGGCTCAAGATCTAAggaagcgggaagagaaaactgggtgcaggaag
601 aggaaactgggtgcaggagcaggaagcagacgaggaagtaggcttagtggtgaaaataaa
661 ataacgcggtagtaaggaggaaattgagagaggagtaagaggagacaggaaggaaacat
721 gaggttggtgataagccagtcataaaaaacttgactttccagagagaacagcagcccat
781 gacaaggaaatttataaagtgatagagaagtaaaggtagacgagaatgatacgaataata
841 aagtgttgaacaaagctaaaaaaaaaaaaaaaaaaaaaaaaaaaaaaaaaaaaaaaaaaaa
901 aaaaaaaaaaaaaaaaaaaaaaaaaaaaaaaaaaaaaaaaaaaaaaaaaaaaaaaaaaaaaa

```

Figure 1. Nucleotide and deduced amino acid sequences of EsALF-3. The asterisk (*) indicates the stop codon. The putative signal peptide is underlined.

The potential tertiary structures of EsALF-3

The potential tertiary structure of EsALF-3 was established using the SWISS-MODEL prediction algorithm based on the template 2jobA (Figure 4). It comprises an N-terminal α -helix, a simple four-stranded anti-parallel β -sheet and two C-terminal α -helices. Strands 2 and 3 of the β -sheet are connected at the bottom by a disulfide bond (Cys55-Cys76) forming a hairpin loop.

Tissue distribution of EsALF-3 mRNA

Quantitative real-time RT-PCR was employed to quantify mRNA expression of EsALF-3 in the tissues of healthy crabs, including haemocytes, hepatopancreas, muscle,

gonad, gill and heart (Figure 5). For both EsALF-3 and β -actin genes, there was only one peak at the corresponding melting temperature in the dissociation curve analysis, indicating that the PCR was specifically amplified. The mRNA transcripts of EsALF-3 could be detected in all the examined tissues with significant variation of expression level. The highest expression level of EsALF-3 was observed in haemocytes, while the lowest expression level was found in heart, which was only 0.04-fold ($P < 0.01$) compared to the expression level in haemocytes. The moderate expression levels were observed in hepatopancreas, muscle, gonad and gill.

Recombinant expression of EsALF-3 in *E. coli*

The recombinant plasmid pET-32a-EsALF-3 was trans-

Fig. 2

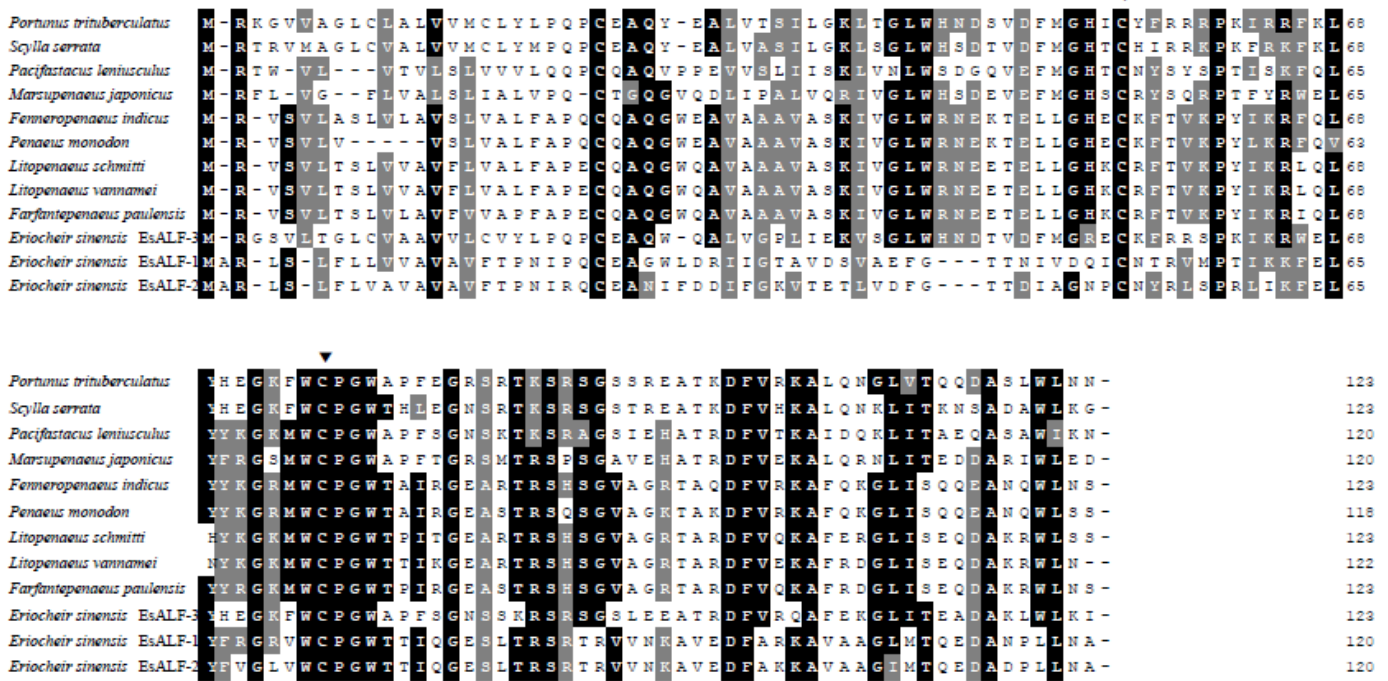


Figure 2. Multiple alignment of EsALF-3 with other known ALFs. Amino acid residues that are conserved in at least 60 % of sequences are shaded in dark, and similar aminoacids are shaded in grey. The species and the GenBank accession numbers are as follow: *E. sinensis* EsALF-1 (ABG82027), *Eriocheir sinensis* EsALF-2 (ACY25186), *Portunus trituberculatus* (ACM89169), *Scylla serrata* (ACH87655), *Pacifastacus leniusculus* (ABQ12866), *Marsupenaeus japonicus* (BAH22585), *Fenneropenaeus indicus* (ADE27980), *Penaeus monodon* (ACC86067), *Litopenaeus schmitti*(ABJ90465), *Litopenaeus vannamei* (ACT21197), *Farfantepenaeus paulensis* (ABQ96193). Conserved cysteine residues are marked with ▼.

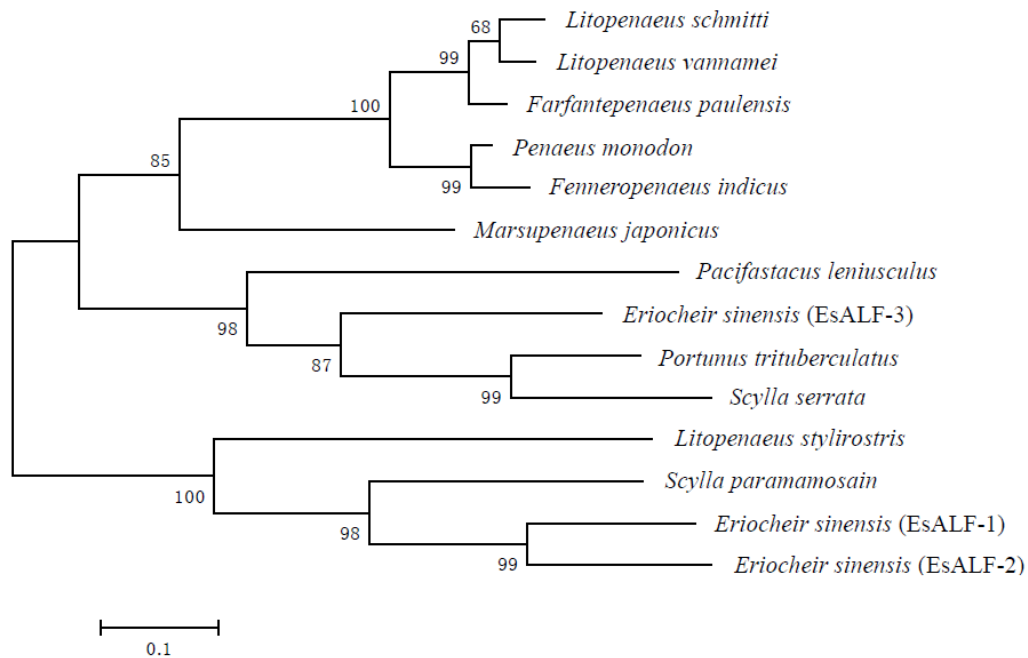


Figure 3. Consensus neighbour-joining tree based on the sequences of ALFs from crustaceans. The numbers at the forks indicate the bootstrap. The detailed information of ALFs from *E. sinensis*, *P. trituberculatus*, *S. serrata*, *P. leniusculus*, *M. japonicus*, *F. indicus*, *P. monodon*, *L. schmitti*, *L. vannamei* and *F. paulensis* are indicated in Figure 2. The GenBank accession numbers for ALFs from *L. stylirostris* and *S. paramamosain* are AAY33769 and ADT71677, respectively.

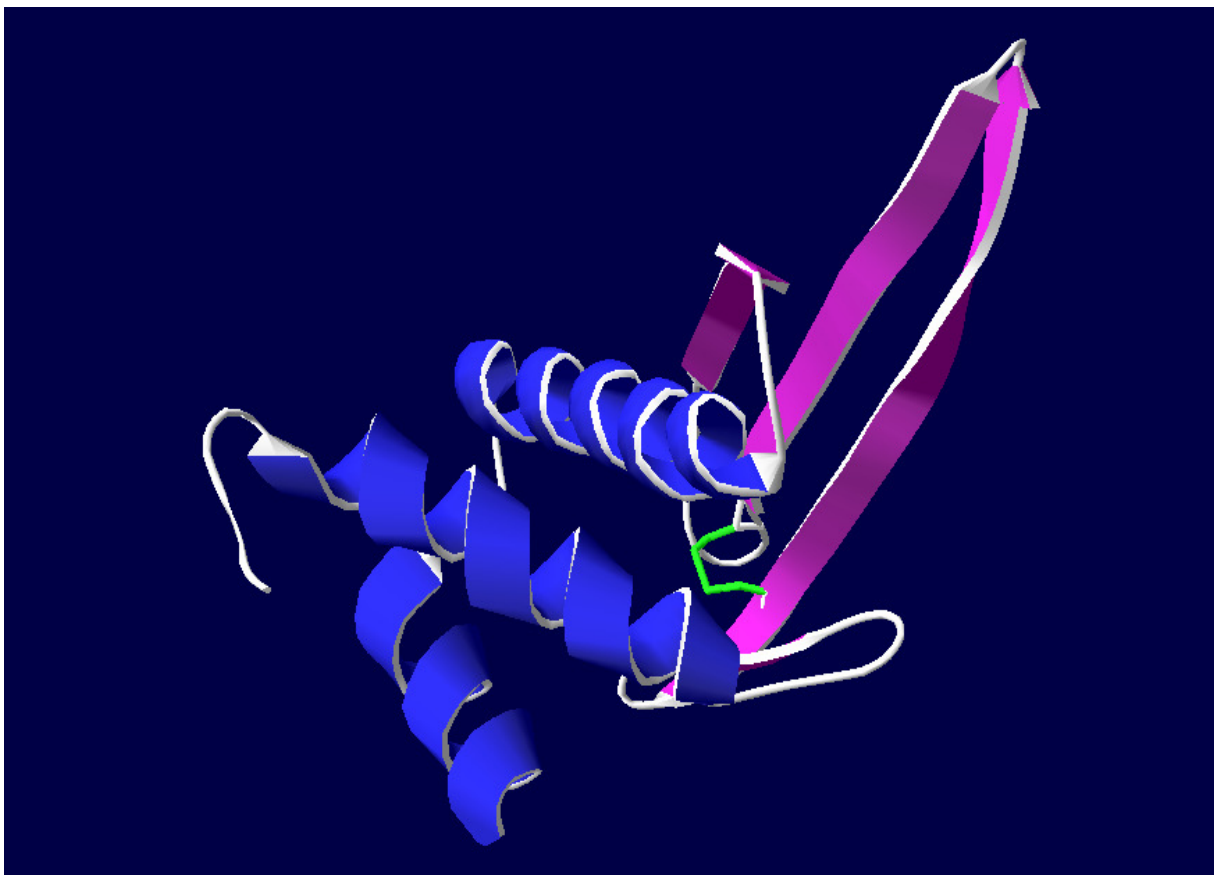


Figure 4. The predicted spatial structure of EsALF-3 predicted by SWISS-MODEL program. Blue: α -helices; Purple: β -strand and white: random coil. There are an N-terminal α -helix, a simple four-stranded anti-parallel β -sheet and two C-terminal α -helices. The two conserved cysteine residues of EsALF-3 forming a disulfide bond are colored in green in Strands 2 and 3 of the β -sheet.

formed and expressed in *E. coli* BL21(DE3)-pLysS. After IPTG induction for 4 h, the whole cell lysate was analyzed by SDS-PAGE, and a distinct band was revealed with a molecular weight of 32 kDa (Figure 6), which was in accordance with the predicted molecular mass. The rEsALF-3 protein was quantified and the concentration was $540 \mu\text{g mL}^{-1}$.

Antimicrobial activity of rEsALF-3

The purified recombinant protein of EsALF-3 displayed antibacterial activity against Gram-negative bacteria *L. anguillarum* and *E. coli*, and Gram-positive bacterium *B. subtilis* (Figure 7), but no obvious antifungal activity against *P. pastoris* was observed. After overnight incubation, the absorbance of the culture in each well for bacterial was determined using a precision micro-plate reader at 600 nm. For Gram-negative bacteria *L. anguillarum*, the absorbances of the wells were 0.05 ± 0.001 (mean \pm S.E.), 0.06 ± 0.006 and 0.09 ± 0.011 in rEsALF-3-treatment group, rTRX-treatment group and blank group, respectively and OD_{600} of rEsALF-3-

treatment group was remarkably lower ($P < 0.01$) than those of blank group and rTRX-treatment group. For another Gram-negative bacteria *E. coli*, the 0.40 ± 0.014 absorbance was observed in rEsALF-3-treatment group, which was significantly lower ($P < 0.01$) than those of blank group (0.62 ± 0.033) and rTRX-treatment group (0.55 ± 0.053). For Gram-positive bacteria *B. subtilis*, the absorbance value of rEsALF-3-treatment group was also significantly lower ($P < 0.01$) than those of blank and rTRX-treatment group, and the absorbance values in rEsALF-3-treatment group, blank group, rTRX treatment group were 0.24 ± 0.004 , 0.44 ± 0.057 and 0.38 ± 0.060 , respectively. The MIC of the rEsALF-3 for *L. anguillarum*, *E. coli* and *B. subtilis* were $33.75 \mu\text{g mL}^{-1}$, $270 \mu\text{g mL}^{-1}$ and $135 \mu\text{g mL}^{-1}$, respectively (Figure 8).

DISCUSSION

As an important member of AMP family, ALF can bind and neutralize lipopolysaccharide (LPS), mediating degranulation and activation of an intracellular coagulation cascade (Morita et al., 1985; Warren et al., 1992).

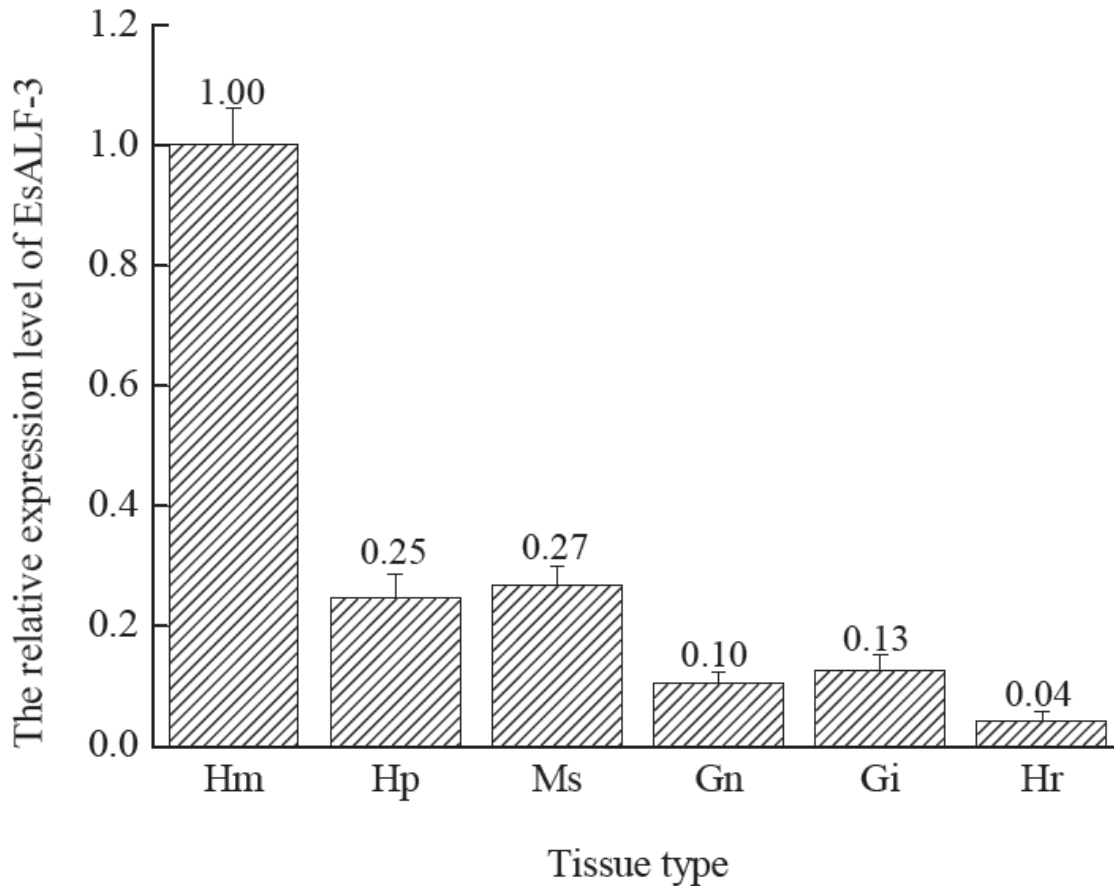


Figure 5. Real-time PCR analysis of the EsALF-3 gene transcripts relative to β -actin transcripts of crabs at six different tissues. Hm-haemocytes, Hp-hepatopancreas, Ms-muscle, Gn-gonad, Gi-gill and Hr-heart. EsALF-3 transcript level in hepatopancreas, muscle, gonad, gill and heart is normalized to that in haemocytes. All the data are analyzed from five individuals. Vertical bars represent the mean \pm S.E. (N = 5).

Different ALF isoforms can coexist in one organism and display different biological activities to protect organism from different pathogens. For example, two distinct ALF (LvALF1 and LvALF2) were constitutively expressed in different tissues of *L. vannamei*, which were presumed to represent different antimicrobial activities (de la Vega et al., 2008). In the present study, the third ALF gene was cloned from *E. sinensis*, which was designated as EsALF-3 to distinguish EsALF-1 and EsALF-2 identified in our previous study (Li et al., 2008; Zhang et al., 2010b). The full-length cDNA of EsALF-3 contained an open reading frame (ORF) of 369 bp encoding a polypeptide of 123 amino acids (Figure 1). The deduced amino acid sequence of EsALF-3 displayed higher similarities to two ALFs from other crabs *P. trituberculatus* (67% similarity) and *S. serrata* (61% similarity), while lower similarities to EsALF-1 (40%) and EsALF-2 (41%). There were two conserved cysteine residues in EsALF-3 (Figure 2), which were highly conserved in all the ALFs and involved in forming the disulfide bridges to stabilize the ALFs 3D structure (Yang et al., 2009). A phylogenetic tree was constructed based on the amino acid sequence

of EsALF-3 and ALFs from shrimps and crabs (Figure 3). The EsALF-3 was closer matched to ALFs from crabs *P. trituberculatus* and *S. serrata*, but relatively farther from EsALF-1 and EsALF-2, implying that EsALF-3 was a new ALF in *E. sinensis*. The sequence character and phylogenetic relationship also promise the potential difference in biological activities of EsALF-3 comparison with EsALF-1 and EsALF-2.

The spatial structure of EsALF-3 was established using the SWISS-MODEL prediction algorithm based on the template 2jobA (Arnold et al., 2006). There were three α -helices and four β -strands in the spatial structure of EsALF-3, and two conserved-cysteine residues (C⁵⁵ and C⁷⁶) at the bottom of strands 2 and 3 of the β -sheet formed a disulfide bond that constrained a hairpin loop (Figure 4). The hairpin loop was recognized as the potential lipid A (LPS)-binding site, which was highly conserved in ALF family, and mainly consisted of 5 to 6 positively charged residues and several hydrophobic residues forming an amphipatic loop structure (Yang et al., 2009). The amphipatic loop structure was believed to bind a single fatty acid with the phosphoglucosamine portion of

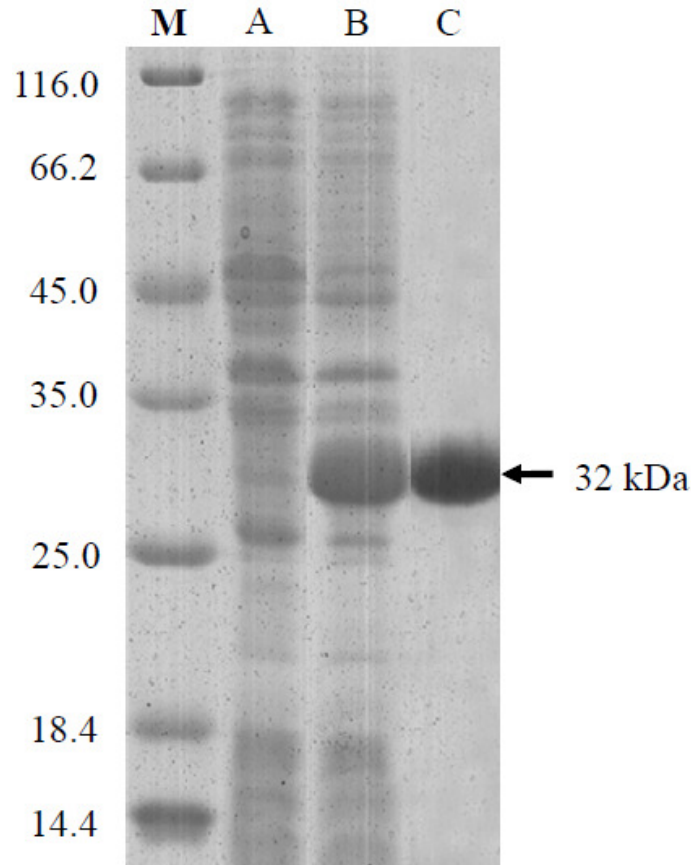


Figure 6. SDS-PAGE analysis of rEsALF-3. M: Protein molecular weight standards (kDa); Lane A: negative control for rEsALF-3 (without induction); lane B: IPTG induced rEsALF-3; lane C: purified rEsALF-3. The molecular weight of rEsALF-3 was 32 kDa.

lipid A (Nagoshi et al., 2006). The presence of lipid A (LPS)-binding site in EsALF-3 indicated that EsALF-3 could bind and neutralize LPS and play a role in protecting crabs from pathogen invasion. All the three ALFs from *E. sinensis* had the amphipatic loop structure with the lipid A (LPS)-binding site which located on the strands 2 and 3 of the β -sheet. It was notable that there were three α -helices in EsALF-1 and EsALF-3, while only two α -helices in EsALF-2. Moreover, multiple alignment revealed that the number of the positively charged residue and hydrophobic residue in the lipid A (LPS)-binding site of three EsALFs was different, especially the number of the positively charged residues (Figure 2). The differences of the EsALFs in their spatial structures and the amino acid sequences of lipid A (LPS)-binding site implied that they might perform different antimicrobial spectrum and different antimicrobial activity in the immune system of *E. sinensis*.

The distribution of EsALF-3 mRNA in different tissues was detected by quantitative real-time PCR to survey its potential venues of biological activity. The EsALF-3 mRNA was expressed in all the examined tissues,

including haemocytes, hepatopancreas, muscle, gonad, gill and heart of unchallenged crabs (Figure 5). This expression profile was in agreement with that of ALFs from *F. chinensis* (Liu et al., 2005), *M. japonicus* (Nagoshi et al., 2006), *S. serrata* (Yedery and Reddy, 2009) and *P. trituberculatus* (Yue et al., 2010). In our previous study, EsALF-1 was only constitutively expressed in haemocytes, heart and gonad, and had high levels of expression in haemocytes (Li et al., 2008). EsALF-2 mRNA was detected at high levels in gill and muscle, and moderate levels in haemocytes and hepatopancreas, while lowest levels in gonad and heart (Zhang et al., 2010b). Unlike EsALF-1, EsALF-3 was constitutively expressed in all the examined tissues, with moderate expression levels in hepatopancreas and muscle (Figure 5). The different tissue distribution pattern of these two EsALFs suggested that they could provide protective functions against pathogens in different tissues. Meanwhile, the universal distribution of EsALF-3 mRNA also gave a hint that it was involved in a broader scope of protection. Compared with EsALF-2, EsALF-3 was highest expressed in haemocytes and relatively lower expressed in gill (Figure

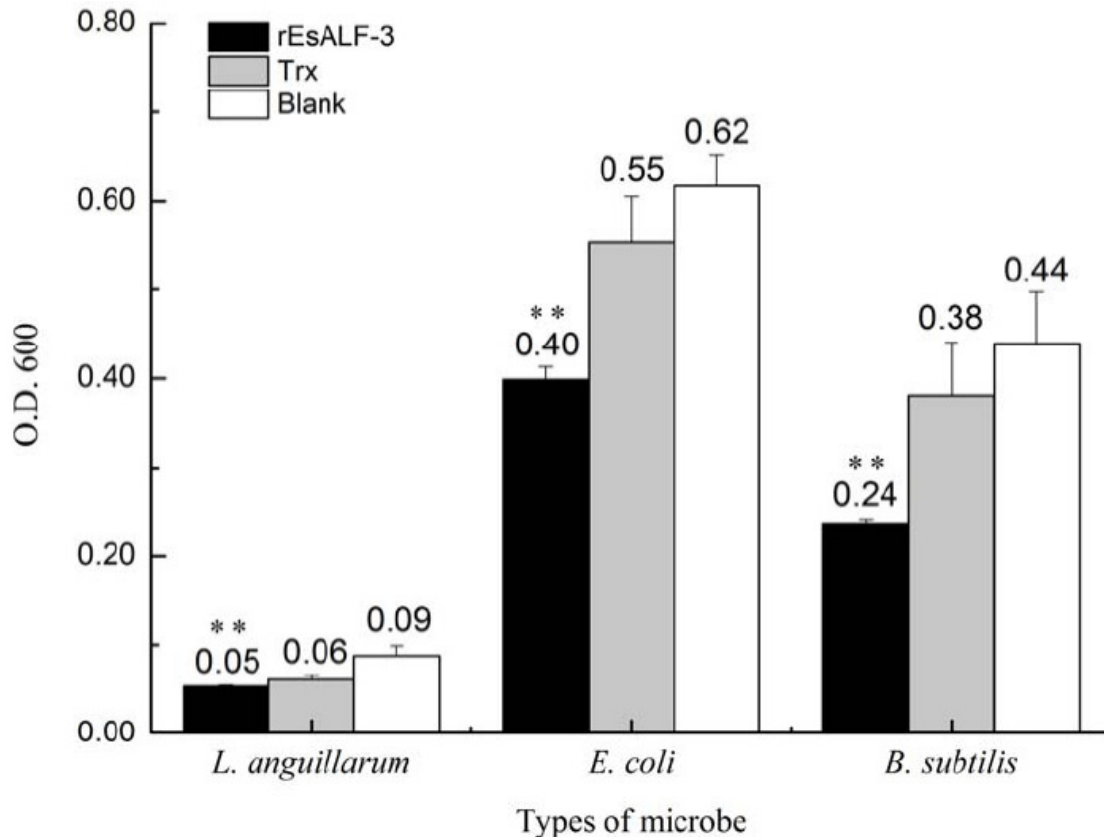


Figure 7. Absorbance at 600nm for *L. anguillarum*, *E. coli* and *B. subtilis* in rEsALF-3 group (black bars), rTRX group (grey bars) and blank group (white bars), respectively. Vertical bars represent the mean \pm S.E. (N= 4). Significant differences between challenged and control group are indicated with two asterisks at $P < 0.01$.

5). In crustacean species, haemocytes are systemically circulated and considered to play extremely important roles in immune defense not only by direct sequestration and killing of foreign invaders, but also by synthesis and exocytosis of bioactive molecules (Beale et al., 2008, Roch, 1999). The highest EsALF-3 mRNA level in haemocytes implied that the hemocytes were the main site to produce EsALF-3, and the EsALF-3 protein secreted by circulated hemocytes could directly participate in the prevention of microbial exploitation in different tissues. All these results together suggested that EsALF-3 was a broad distributing molecule involved in the host immune defense, and might have a prior protection role compared with EsALF-1 and EsALF-2 in *E. sinensis*.

In order to evaluate its antimicrobial activity, the mature peptide of EsALF-3 was expressed in *E. coli* (DE3)-pLysS. The recombinant protein (rEsALF-3) exhibited broad-spectrum antimicrobial activity towards Gram-positive and Gram-negative bacteria. The MIC of rEsALF-3 against *L. anguillarum*, *E. coli* and *B. subtilis* were $33.75 \mu\text{g mL}^{-1}$, $270 \mu\text{g mL}^{-1}$ and $135 \mu\text{g mL}^{-1}$, respectively (Figures 7 and 8). In our previous study, EsALF-1 was found to have the antimicrobial activity against Gram-negative bacteria *L. anguillarum* and *E. coli*, and Gram-positive bacteria *M.*

luteus, while EsALF-2 displayed antimicrobial activity against Gram-negative bacteria *L. anguillarum* and yeast *P. pastoris* (Li et al., 2008; Zhang et al., 2010b). Even though EsALF-3 and EsALF-1 both exhibited broad-spectrum antimicrobial activity towards Gram-negative and Gram-positive bacteria, the antimicrobial activity of EsALF-1 was relatively weak against Gram-negative bacteria (Li et al., 2008). Except for the antimicrobial activity against Gram-positive, the MIC of antimicrobial rEsALF-3 for Gram-negative bacteria *L. anguillarum* ($33.75 \mu\text{g mL}^{-1}$) was much lower than that of the rEsALF-2 ($75 \mu\text{g mL}^{-1}$) (Zhang et al., 2010b). The stronger antimicrobial activity for Gram-negative bacteria *L. anguillarum* might be explained by the special structure of the LPS-binding site of EsALF-3. The Lipid A (LPS)-binding site of ALF is a β -sheet structure and mainly consists of 5 to 6 positively charged residues and several hydrophobic residues to interact through electrostatic and hydrophobic interactions with the lipid A moiety (Yang et al., 2009). The EsALF-3 contained a potential LPS-binding site of 22 amino acid residues which located between two conserved cysteine residues (C⁵⁵ and C⁷⁶) and forming a positively charged amphipathic hairpin loop. There were eight positively charged amino acid residues

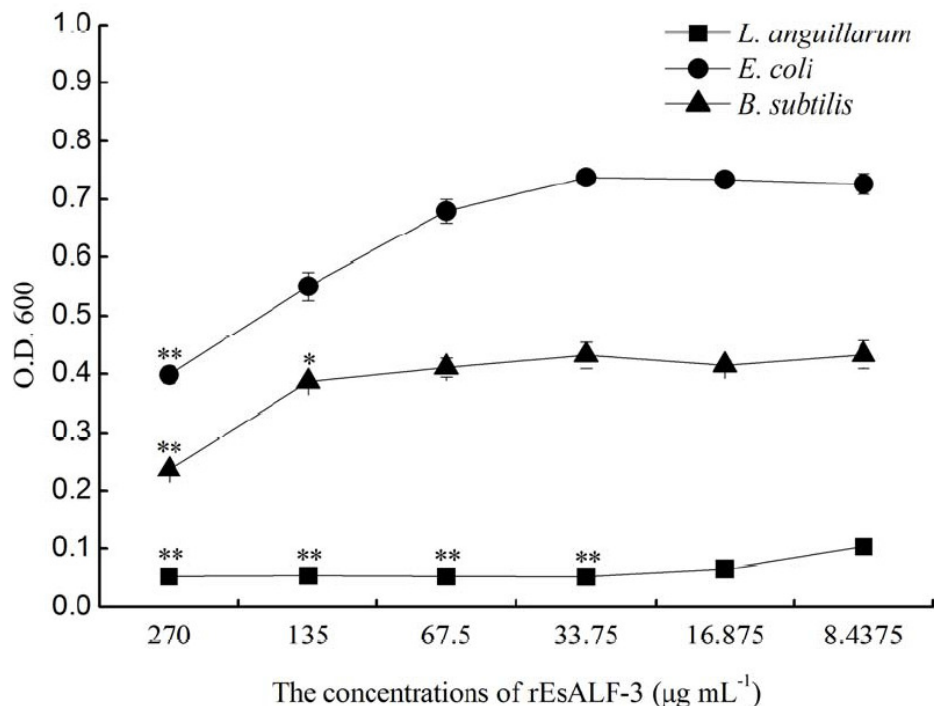


Figure 8. The relationships of absorbance at 600nm for *L. anguillarum*, *E. coli* and *B. subtilis* and 1/2-fold serial diluted concentrations of rEsALF-3. Vertical bars represent the mean \pm S.E. (N = 4). Significant differences between challenged and control group are indicated with an asterisk at P < 0.05, and with two asterisks at P < 0.01.

(K⁵⁶, R⁵⁸, R⁵⁹, K⁶², K⁶⁴, R⁶⁵, H⁷⁰ and K⁷³) in the hairpin loop of EsALF-3, while only three (R³⁰, R³⁴ and K³⁷) in EsALF-1 and five (R³⁰, K³⁶, K³⁷, R⁴³ and R⁴⁵) in EsALF-2 (Li et al., 2008, Zhang et al., 2010b). The more positively charged amino acid in EsALF-3 might contribute to the stronger interaction with the anionic region of LPS and the more forceful antimicrobial activities. No obvious antifungal activity was observed against yeast *P. pastoris* in rEsALF-3-treatment group, which was similar to most ALFs characterized in crustacean species, such as ALFs from *S. paramamosain* (Imjongjirak et al., 2007), *Homarus americanus* (Beale et al., 2008) and *S. serrata* (Yedery and Reddy, 2009). Considering the difference of activity and the antimicrobial spectrums as well as the tissue distribution of their mRNA, it was speculated that EsALF-3 and two other EsALFs (EsALF-1 and EsALF-2) might collectively involve in crab immunity against various pathogens, and perform antibacterial activities for some special pathogens either with cooperation or solo performance.

In conclusion, a new ALF with antibacterial activities was characterized from *E. sinensis* (EsALF-3). The activities and antimicrobial spectrum of EsALF-3 was different from those of the previous reported ALFs (EsALF-1 or EsALF-2). The multiple ALF variants coexist in *E. sinensis* may suggest that Chinese mitten crab, as an invertebrate, relies on the diversity of germ-line encoded immune effector molecules in innate

immune system, such as ALF, to deal with various pathogens in the aquatic environment, meanwhile, this immune defense strategy, to some extent, offset the deficiency of the adaptive immune system in invertebrate.

ACKNOWLEDGEMENTS

The authors are grateful to Dr. Zhaolan Mo and Dr. Zhaoxia Cui from Institute of Oceanology for the kind provision of *L. anguillarum*, *B. subtilis* and sample collection. This research was supported by National Basic Research Program of China (973 program, No. 2012CB114405) from the Chinese Ministry of Science and Technology, a common weal project (No. nyhyzx07-047) from the Chinese Ministry of Agriculture.

REFERENCES

- Arnold K, Bordoli L, Kopp J, Schwede T (2006). The SWISS-MODEL workspace: a web-based environment for protein structure homology modelling. *Bioinformatics*, 22: 195-201.
- Bachere E, Gueguen Y, Gonzalez M, de Lorgeril J, Garnier J, Romestand B (2004). Insights into the anti-microbial defense of marine invertebrates: the penaeid shrimps and the oyster *Crassostrea gigas*. *Immunol. Rev.* 198: 149-168.
- Beale KM, Towle DW, Jayasundara N, Smith CM, Shields JD, Small HJ, Greenwood SJ (2008). Anti-lipopolysaccharide factors in the American lobster *Homarus americanus*: Molecular characterization and transcriptional response to *Vibrio fluvialis* challenge. *Comp.*

- Biochem. Physiol. Part D: Genomics Proteomics, 3: 263-269.
- Boman H (1995). Peptide antibiotics and their role in innate immunity. *Annu. Rev. Immunol.* 13: 61-92.
- Boman HG (2003). Antibacterial peptides: basic facts and emerging concepts. *J. Int. Med.* 254: 197-215.
- Bulet P, Stocklin R, Menin L (2004). Anti-microbial peptides: from invertebrates to vertebrates. *Immunol. Rev.* 198: 169-184.
- de la Vega E, O'Leary NA, Shockey JE, Robalino J, Payne C, Browdy CL, Warr GW, Gross PS (2008). Anti-lipopolsaccharide factor in *Litopenaeus vannamei* (LvALF): A broad spectrum antimicrobial peptide essential for shrimp immunity against bacterial and fungal infection. *Mol. Immunol.* 45: 1916-1925.
- Destoumieux D, Bulet P, Loew D, VanDorsseleer A, Rodriguez J, Bachere E (1997). Penaeidins, a new family of antimicrobial peptides isolated from the shrimp *Penaeus vannamei* (decapoda). *J Biol Chem.* 272: 28398-28406.
- Gai YC, Wang LL, Zhao JM, Qiu LM, Song LS, Li L, Mu CK, Wang W, Wang MQ, Zhang Y, Yao XM, Yang JL (2009). The construction of a cDNA library enriched for immune genes and the analysis of 7535 ESTs from Chinese mitten crab *Eriocheir sinensis*. *Fish. Shellfish Immunol.* 27: 684-694.
- Hancock REW (1997). Peptide antibiotics. *Lancet*, 349: 418-422.
- Hoess A, Watson S, Siber GR, Liddington R (1993). Crystal structure of an endotoxin-neutralizing protein from the horseshoe crab, Limulus anti-LPS factor, at 1.5 Å resolution. *EMBO J.* 12: 3351-3356.
- Hoffmann JA, Kafatos FC, Janeway CA, Ezekowitz RA (1999). Phylogenetic perspectives in innate immunity. *Science*, 284: 1313-1318.
- Imjongjirak C, Amparyup P, Tassanakajon A, Sittipraneed S (2007). Antilipopolsaccharide factor (ALF) of mud crab S. paramamosain: molecular cloning, genomic organization and the antimicrobial activity of its synthetic LPS binding domain. *Mol. Immunol.* 44: 3195-3203.
- Jenssen H, Hamill P, Hancock RE (2006). Peptide antimicrobial agents. *Clin Microbiol. Rev.* 19: 491-511.
- Khoo L, Robinette DW, Noga EJ (1999). Callinectin, an Antibacterial Peptide from Blue Crab, *Callinectes sapidus*, Hemocytes. *Mar. Biotechnol.* (NY). 1: 44-51.
- Laemmli UK (1970). Cleavage of structural proteins during the assembly of the head of bacteriophage T4. *Nature*, 227: 680-685.
- Li CH, Zhao JM, Song LS, Mu CK, Zhang H, Gai YC, Qiu LM, Yu YD, Ni DJ, Xing KZ (2008). Molecular cloning, genomic organization and functional analysis of an anti-lipopolsaccharide factor from Chinese mitten crab *Eriocheir sinensis*. *Dev. Comp. Immunol.* 32: 784-794.
- Liu F, Liu Y, Li F, Dong B, Xiang JH (2005). Molecular cloning and expression profile of putative antilipopolsaccharide factor in Chinese shrimp (*Penaeus chinensis*). *Mar. Biotechnol* (NY). 7: 600-608.
- Morita T, Ohtsubo S, Nakamura T, Tanaka S, Iwanaga S, Ohashi K, Niwa M (1985). Isolation and biological activities of limulus anticoagulant (anti-LPS factor) which interacts with lipopolysaccharide (LPS). *J. Biochem.* 97: 1611-1620.
- Nagoshi H, Inagawa H, Morii K, Harada H, Kohchi C, Nishizawa T, Taniguchi Y, Uenobe M, Honda T, Kondoh M (2006). Cloning and characterization of a LPS-regulatory gene having an LPS binding domain in kuruma prawn *Marsupenaeus japonicus*. *Mol. Immunol.* 43: 2061-2069.
- Relf JM, Chisholm JRS, Kemp GD, Smith VJ (1999). Purification and characterization of a cysteine-rich 11.5-kDa antibacterial protein from the granular haemocytes of the shore crab, *Carcinus maenas*. *Eur. J. Biochem.* 264: 350-357.
- Ried C, Wahl C, Miethke T, Wellenhofer G, Landgraf C, Schneider-Mergener J, Hoess A (1996). High affinity endotoxin-binding and neutralizing peptides based on the crystal structure of recombinant Limulus anti-lipopolsaccharide factor. *J. Biol. Chem.* 271: 28120-28127.
- Roch P (1999). Defense mechanisms and disease prevention in farmed marine invertebrates. *Aquaculture*, 172: 125-145.
- Rosa RD, Stoco PH, Barracco MA (2008). Cloning and characterisation of cDNA sequences encoding for anti-lipopolsaccharide factors (ALFs) in Brazilian palaemonid and penaeid shrimps. *Fish. Shellfish Immunol.* 25: 693-696.
- Schnapp D, Kemp GD, Smith VJ (1996). Purification and characterization of a proline-rich antibacterial peptide, with sequence similarity to bactenecin-7, from the haemocytes of the shore crab, *Carcinus maenas*. *Eur. J. Biochem.* 240: 532-539.
- Somboonwiwat K, Marcos M, Tassanakajon A, Klinbunga S, Aumelas A, Romestand B, Gueguen Y, Boze H, Moulin G, Bachere E (2005). Recombinant expression and anti-microbial activity of anti-lipopolsaccharide factor (ALF) from the black tiger shrimp *Penaeus monodon*. *Dev. Comp. Immunol.* 29: 841-851.
- Tanaka S, Nakamura T, Morita T, Iwanaga S (1982). Limulus anti-LPS factor: an anticoagulant which inhibits the endotoxin mediated activation of Limulus coagulation system. *Biochem. Biophys. Res Commun.* 105: 717-723.
- Vallespi MG, Alvarez-Obregon JC, Rodriguez-Alonso I, Montero T, Garay H, Reyes O, Arana MJ (2003). A Limulus anti-LPS factor-derived peptide modulates cytokine gene expression and promotes resolution of bacterial acute infection in mice. *Int Immunopharmacol.* 3: 247-256.
- Vallespi MG, Glaria LA, Reyes O, Garay HE, Ferrero J, Arana MJ (2000). A Limulus antilipopolsaccharide factor-derived peptide exhibits a new immunological activity with potential applicability in infectious diseases. *Clin. Diagn. Lab. Immunol.* 7: 669-675.
- Wang W, Chen J, Du K, Xu Z (2004). Morphology of spiroplasmas in the Chinese mitten crab *Eriocheir sinensis* associated with tremor disease. *Res. Microbiol.* 155: 630-635.
- Wang W, Gu Z (2002). Rickettsia-like organism associated with tremor disease and mortality of the Chinese mitten crab *Eriocheir sinensis*. *Dis Aquat Organ.* 48: 149-153.
- Warren HS, Glennon ML, Wainwright N, Amato SF, Black KM, Kirsch SJ, Riveau GR, Whyte RI, Zapol WM, Novitsky TJ (1992). Binding and neutralization of endotoxin by Limulus antilipopolsaccharide factor. *Infect Immun.* 60: 2506-2513.
- Wu HX, Feng MG (2004). Mass mortality of larval *Eriocheir sinensis* (Decapoda: Grapsidae) population bred under facility conditions: possible role of Zoothamnium sp (Peritrichida: Vorticellidae) Epiphyte. *J Invertebr Pathol.* 86: 59-60.
- Yang Y, Boze H, Chemardin P, Padilla A, Moulin G, Tassanakajon A, Pugnieri M, Roquet F, Destoumieux-Garzon D, Gueguen Y, Bachere E, Aumelas A (2009). NMR structure of rALF-Pm3, an anti-lipopolsaccharide factor from shrimp: model of the possible lipid A-binding site. *Biopolymers*, 91: 207-220.
- Yedery RD, Reddy KVR (2009). Identification, cloning, characterization and recombinant expression of an anti-lipopolsaccharide factor from the hemocytes of Indian mud crab, *Scylla serrata*. *Fish Shellfish Immunol.* 27: 275-284.
- Ying X, Yang W, Zhang Y (2006). Comparative studies on fatty acid composition of the ovaries and hepatopancreas at different physiological stages of the Chinese mitten crab. *Aquaculture*, 256: 617-623.
- Yue F, Pan LQ, Miao JJ, Zhang L, Li J (2010). Molecular cloning, characterization and mRNA expression of two antibacterial peptides: Crustin and anti-lipopolsaccharide factor in swimming crab *Portunus trituberculatus*. *Comp Biochem Physiol B: Biochem. Mol. Biol.* 156: 77-85.
- Zhang Y, Song LS, Zhao JM, Wang LL, Kong PF, Liu L, Wang MQ, Qiu LM (2010a). Protective immunity induced by CpG ODNs against white spot syndrome virus (WSSV) via intermediation of virus replication indirectly in *Litopenaeus vannamei*. *Dev Comp Immunol.* 34: 418-424.
- Zhang Y, Wang LL, Wang LL, Yang JL, Gai YC, Qiu LM, Song LS (2010b). The second anti-lipopolsaccharide factor (EsALF-2) with antimicrobial activity from *Eriocheir sinensis*. *Dev. Comp. Immunol.* 34: 945-952.
- Zhang SY, Zhang JH, Huang CH, Jean Robert B, Shi ZL (2002). Preliminary Studies on Two Strains of Reovirus from Crab *Eriocheir sinensis*. *Virologica Sinica*, 17: p. 5.